

Study of the Reaction $\text{Ne}^{20}(\alpha, \alpha'\gamma)\text{Ne}^{20*}\dagger$

W. W. EIDSON AND R. D. BENT

Department of Physics, Indiana University, Bloomington, Indiana

(Received June 25, 1962)

Particle-gamma coincidence spectra of the reaction $\text{Ne}^{20}(\alpha, \alpha'\gamma)\text{Ne}^{20}$ provide evidence for the existence of two, new, gamma-emitting levels in Ne^{20} . A new level at 7.93 MeV is observed to decay by gamma emission to the 4.97-MeV (2^-) level; a new level at 5.88 MeV is observed to decay to the 4.25-MeV (4^+) level. Tentative spin-parity assignments are 3^+ for the 5.88-MeV level and 1^+ , 2^- , 3^+ , or 4^- for the 7.93-MeV level. Evidence is seen for the recently discovered level at 7.02 MeV (4^-). The data suggest a considerably larger value of Γ_γ/Γ for the 5.63-MeV (3^-) level than that previously reported. Angular distribution measurements of elastic and inelastic alpha-particle groups are compared with current direct-interaction theory. The production of states of Ne^{20} with $J \neq L$ through inelastic alpha-particle scattering suggests a fairly strong spin-orbit interaction between the orbital angular momentum of the incident alpha particle and the spin of one (or more) target nucleons. Possible collective model interpretations of the Ne^{20} level structure are suggested.

I. INTRODUCTION

FROM the standpoint of nuclear models, Ne^{20} is an especially interesting nucleus. The success of the alpha-particle model¹ in describing O^{16} suggests that this model may also have some validity for Ne^{20} . Elliott and Flowers² have pointed out that it is feasible to describe in detail the low-lying levels of Ne^{20} by intermediate coupling shell-model calculations. Rakavy³ predicts that nuclei in the region of Ne^{20} should have large deformations and, therefore, exhibit rotational spectra. A preliminary attempt has been made by Litherland *et al.*⁴ to arrange the low-lying levels of Ne^{20} into overlapping rotational bands. It appears that careful experimental and theoretical studies of Ne^{20} may lead to a better understanding of the validity and interrelation of different nuclear models.

The present experiments were undertaken to search for unnatural parity [$\pi \neq (-1)^J$] states of Ne^{20} in the energy range from about 5 to 9 MeV. At the time these experiments were begun, no unnatural parity states were known in this energy range, although eleven natural parity [$\pi = (-1)^J$] states were known^{5,6} from resonances in the reaction $\text{O}^{16} + \alpha$. Unnatural parity states cannot be formed in the $\text{O}^{16} + \alpha$ reaction if spin and parity are conserved.

It was not clear at the start whether unnatural parity states in Ne^{20} could be formed with measurable intensity by inelastic scattering of alpha particles if the interaction mechanism were purely direct. The fact that several unnatural parity states were readily formed in the present (α, α') experiments [and also in the (α, α')

experiments of Seidlitz, Bleuler, and Tendam⁷ at 18-MeV bombarding energy] suggests some interesting speculations concerning the reaction mechanism for alpha-particle scattering. [See Sec. III A (d), and discussion.]

II. APPARATUS AND PROCEDURES

Gamma radiation from Ne^{20} was studied employing the $\text{Ne}^{20}(\alpha, \alpha'\gamma)\text{Ne}^{20}$ reaction with the 22-MeV alpha-particle beam of the Indiana University cyclotron. Standard fast-slow coincidence circuitry was arranged so that gamma rays could be studied in time coincidence with charged reaction particles of a selected energy. In this way, it was possible to study the decay modes of individual levels or to search for new levels when these levels decayed predominately by gamma-ray emission. As a check on the interpretation of the coincidence gamma-ray spectra, measurements were also made of charged-particle spectra in time coincidence with gamma rays of a selected energy. Angular distribution measurements were made on the elastic and inelastic groups resolved by the particle detector in order to determine optimum scattering angles for the particle-gamma coincidence measurements.

Figure 1 shows the experimental area. The cyclotron beam was focused by two, small quadrupole lenses located in the cyclotron vault; it then passed through collimator "A" shown in Fig. 1, through the analyzing magnet, and finally through collimators "B" and "C" before entering the gamma-ray hut. Collimator "D" contained three "antiscatter" apertures which were larger in diameter than collimator "C"; these apertures did not define the main part of the beam but prevented scattered particles not traveling parallel to the beam pipe from entering the scattering chamber. All collimators were constructed of high-Z materials (lead or tantalum) to minimize gamma-ray background produced when 22-MeV alpha particles strike the collimators. All collimators which define the beam spot were located outside the 15-in.-thick concrete gamma-ray hut; at least

* Supported by the Office of Naval Research.

† A preliminary report of this work was given at the Washington meeting of the American Physical Society, 1961. [W. W. Eidson, R. D. Bent, and R. A. LaSalle, *Bull. Am. Phys. Soc.* **6**, 249 (1961).]

¹ D. M. Dennison, *Phys. Rev.* **96**, 378 (1954); S. L. Kameny, *ibid.* **103**, 358 (1956).

² J. P. Elliott and B. H. Flowers, *Proc. Roy. Soc. (London)* **A229**, 536 (1955).

³ G. Rakavy, *Nuclear Phys.* **4**, 375 (1957).

⁴ A. E. Litherland, J. A. Kuehner, H. E. Gove, M. A. Clark, and E. Almquist, *Phys. Rev. Letters* **7**, 98 (1961).

⁵ J. R. Cameron, *Phys. Rev.* **90**, 839 (1953).

⁶ F. Ajzenberg and T. Lauritsen, *Nuclear Phys.* **11**, 1 (1959).

⁷ L. Seidlitz, E. Bleuler, and D. J. Tendam, *Phys. Rev.* **110**, 682 (1958).

12 in. of lead prevented the gamma-ray detector from directly viewing these collimators. Further, all beam pipe external to the cyclotron vault was lined with $\frac{1}{16}$ -in. lead sheet to prevent scattered alpha particles from making contact with the brass beam pipe. These precautions substantially reduced the gamma ray and neutron background in the scattering area. The magnetic spectrometer shown in Fig. 1 was not used in the present experiment.

Further background reduction was necessary when low-intensity gamma rays were to be studied. The normal, external alpha-particle beam from the cyclotron ($1.0 \mu\text{A}$) was found to be typically 1000 times too intense for coincidence experiments under the extremely low duty-cycle conditions prevailing on the cyclotron. It was not practical to reduce the beam intensity through collimation because of increased background; attempts to reduce the internal beam by adjustment of the arc or plate voltage resulted in unstable cyclotron operation and lower duty cycle. The reduction in beam intensity with resulting reduction in background was accomplished by reducing the size of the emission port in the arc cone and by using little beam-defining collimation on the external beam. This permitted stable cyclotron operation with average beam intensities of about one millimicroampere. With the precautions discussed in this and in the preceding paragraph, background counts in the gamma detector not associated with the target chamber were found to be negligible.

The scattering chamber used in the experiment is shown schematically in Fig. 2. A gas target at a pressure of 13 cm of Hg, contained by 0.00002-in.-thick nickel foils was found to be a usable compromise between foil thickness and pressure. As shown in Fig. 2, the foils were mounted on extension tubes and were located near the center of the scattering chamber so that nontarget gas path would be minimal. The heavy black lines on the figure indicate the lead shielding used to prevent scattered alphas from coming into contact with the brass chamber walls. The lead block "D" shields

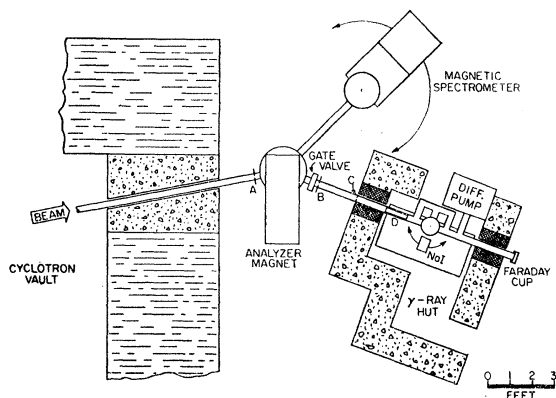


Fig. 1. Cyclotron experimental area including special shielding necessary for low-yield gamma-ray studies.

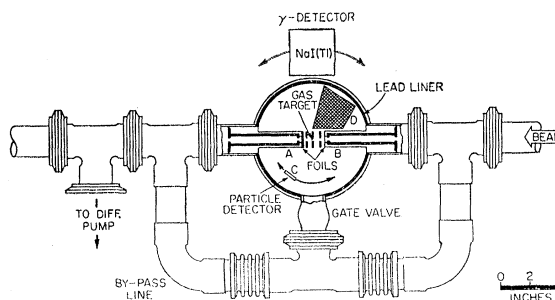


Fig. 2. Details of target chamber used for $\text{Ne}^{20}(\alpha, \alpha'\gamma)\text{Ne}^{20}$ particle-gamma coincidence experiments.

the gamma-ray detector from a direct view of the entrance foil.

Even with these precautions, it was found that 75% of the radiation detected in the gamma-ray detector could be attributed to the nickel foils. A substantial reduction in this background was accomplished by stopping the beam inside the gas-filled chamber on a thick, carefully cleaned lead plate. Lead collimators within the chamber prevented the particle detector from viewing the entrance foil or the lead stopping plate. For the alpha-particle angular distribution measurements, where gamma-ray background was unimportant, the lead plate was easily removed, allowing the beam to pass through the exit foil into the normal beam-integration cup shown in Fig. 1.

Natural neon gas of 99.8% purity was used as the target. The chamber was evacuated by the diffusion pump through the large gate valve to a pressure of 10^{-5} mm of Hg before the gas was admitted to the chamber. The target pressure was monitored by a simple mechanical vacuum gauge which had been calibrated against a manometer. This method proved efficient and satisfactory since absolute cross sections were not of interest in the present experiment.

The particle detector used was a Hughes 1-cm² diffused-junction solid-state detector. The detector was lowered through a port in the lid of the cylindrical scattering chamber, and the detection angle could be changed by rotating the lid on its ball bearing suspension. As the solid-state detector was actually within the gas-filled scattering chamber, careful electrostatic and light shielding was necessary to shield the sensitive detector from the heavy ionization and fluorescence produced when the alpha particles passed through the neon gas. Thin metallic foils work quite well while causing only small degradation of the energy of the alpha particles. The detector was found to be highly stable and reliable at all times.

The gamma-ray detector was a 3- \times 3-in. NaI(Tl) crystal, sealed onto a DuMont type 6363 photomultiplier tube. The entire assembly was mounted outside the vacuum in a dolley which was constrained to rotate about the target volume in the reaction plane. The

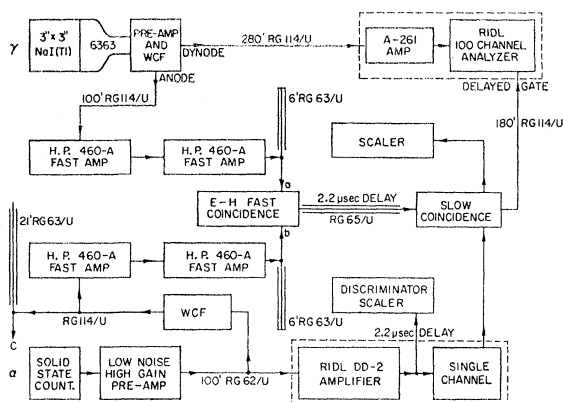


FIG. 3. Block diagram of fast-slow coincidence circuitry used in the experiment. The arrangement shown is for displaying gamma rays in time coincidence with particles of a selected energy.

gamma-ray detector subtended a solid angle of 2.5% of the total sphere.

The detectors described above were used in conjunction with standard fast-slow coincidence circuitry as shown in Fig. 3. This simple arrangement provided the reliability and stability necessary for the long coincidence runs used to study the gamma-ray decay of the Ne^{20} levels. The open-ended 21-ft section of RG 63/U shown in Fig. 3 was used to reduce the 10.6-Mc oscillation on the signal lead which was picked up from the cyclotron oscillator. A fast-coincidence resolving time of about 30 nsec was maintained throughout the experiments. This was sufficient to insure that coincident events occur in the same cyclotron beam pulse.

III. EXPERIMENTAL RESULTS

A. Alpha-Particle Angular Distributions

Prior to the particle-gamma coincidence measurements, angular distributions were measured for the elastic and inelastic alpha-particle groups of interest to determine the optimum scattering angles for the coincidence work. Figure 4 is a typical charged-particle spectrum obtained from the bombardment of natural neon gas with 22-MeV alpha particles. The solid-state detector was collimated to a solid angle of 0.04% of the total sphere and was located at a laboratory scattering angle of 40° . The energy resolution permitted clear identification of the elastic group and the inelastic groups to the 1.63-MeV level (2^+), the 4.25-MeV level (4^+), and the 4.97-MeV level (2^-). The 4.97-MeV group was more clearly resolved at backward angles; at the forward angles, a subtraction technique was used to determine the intensity, so that the relative intensities quoted for the 4.97-MeV group in the forward directions are approximate. The two known levels at⁸ 5.63 and⁹

5.81 MeV were not resolved; the coincidence data to be discussed later imply the existence of a third level at 5.88 MeV which was also unresolved. Groups of levels near 7.2 and 8.8 MeV are seen but not resolved in the present experiment. A detailed discussion of the energy calibration of this spectrum is found elsewhere.¹⁰

The angular distributions measured in the present experiment are shown in Fig. 5. These measurements were taken primarily to determine the scattering angles at which optimum efficiency could be obtained for the $(\alpha, \alpha'\gamma)$ coincidence measurements, and hence absolute differential cross sections were not measured. It is hoped that more accurate differential cross section measurements can be made for 22-MeV alpha particles to complement the precise measurements of Seidlitz, Bleuler, and Tendam⁷ at 18-MeV bombarding energy and to allow more quantitative comparison with direct interaction theory. However, qualitative statements can be made about the elastic and inelastic angular distributions measured in the present experiment.

(a) The sharp diffraction structure observed for the resolved groups indicates a direct reaction mechanism.

(b) The elastic group (0^+) and the inelastic group leaving Ne^{20} excited to 1.63 MeV (2^+) both show the diffraction pattern characteristic of the direct interaction process, and the oscillations are properly out of phase, indicating qualitative agreement with the inelastic diffraction scattering model as calculated in the adiabatic approximation by Blair.¹¹ The patterns are similar to those obtained by Seidlitz, Bleuler, and Tendam⁷ at 18-MeV bombarding energy. A reasonably good fit to the 18-MeV data has been accomplished by Blair,¹¹ using the inelastic diffraction scattering model and it appears that a similarly good fit could be obtained for the 22-

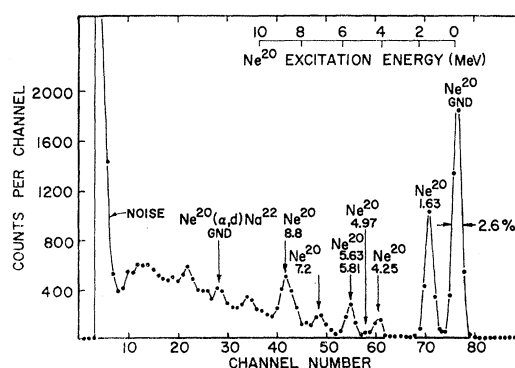


FIG. 4. Charged-particle spectrum from the bombardment of natural neon gas with 22-MeV alpha particles. Spectrum was recorded with a Hughes 1 cm² diffused-junction detector, narrowly collimated for optimum resolution, located at 40° laboratory scattering angle.

⁸ W. W. Buechner and A. Sperduto, Phys. Rev. **106**, 1008 (1957).

⁹ G. M. Temmer, 1961 (private communication). See also H. S. Adams, J. D. Fox, N. P. Heydenburg, and G. M. Temmer, Bull. Am. Phys. Soc. **6**, 250 (1961).

¹⁰ W. W. Eidson, Ph.D. thesis, Indiana University, 1961 (unpublished).

¹¹ J. S. Blair, Phys. Rev. **115**, 928 (1959); J. S. Blair, D. Sharp, and L. Wilets, *ibid.* **125**, 1625 (1962).

MeV data of the present experiment. Such calculations have not been carried out.

(c) The angular distribution of the inelastic group leaving Ne^{20} excited to 4.25 MeV exhibits some structure, but it is not clear whether the pattern is in or out of phase with the elastic group. The data is qualitatively similar to the 18-MeV data of Seidlitz, Bleuler, and Tendam,⁷ but a wider range of angles would be desirable to compare the 22-MeV data of the present experiment with theory and the 18-MeV data. This level has been assigned 4^+ by Gove, Litherland, and Clark¹² and is interpreted by Litherland *et al.*⁴ to be the third member of a $K=0$ rotational band based on the 0^+ ground state.

(d) The 4.97-MeV level of Ne^{20} is thought to have 2^- spin and parity.^{12,13} This requires $J \neq L$ for the 4.97-MeV level, and since both the target and the bombarding particle in the $\text{Ne}^{20}(\alpha, \alpha')$ reaction have zero spin and intrinsically even parity, it seems necessary to assume that if the reaction is purely direct, a strong spin-orbit term is present in the interaction which can "flip" the spin of one or more of the nucleons in the target nucleus, or that the interaction proceeds through a double scattering of the alpha particle. The sharp diffraction structure observed in the angular distribution of the inelastic alpha particles feeding the 4.97-MeV state in this experiment and in the 18-MeV scattering data of Seidlitz, Bleuler, and Tendam⁷ would seem to indicate a direct reaction process. The results of the coincidence spectra, which will be discussed later in this paper, indicate that other unnatural parity levels of Ne^{20} are produced by the inelastic scattering of 22-MeV alpha particles with intensities comparable to the intensities for natural parity levels. It is interesting that the 5.22-MeV (3^+) unnatural parity level of Mg^{24} apparently is produced with very low intensity by the inelastic scattering of 42-MeV alpha particles.¹⁴

(e) Because of the wide apertures used on the solid-state detector, the natural spread of the beam energy (150 keV), and the inherent resolving power of the solid-state detector (100 keV), the levels previously identified at⁸ 5.63 MeV and⁹ 5.81 MeV could not be resolved in this experiment. However, the angular distribution of the sum of the two levels could be easily measured, and is shown in Fig. 5. Spin and parity assignments of 3^- for the 5.63-MeV level and 1^- for the 5.81-MeV level have recently been made by Kuehner.¹⁵ The lack of diffraction structure in the angular distribution is somewhat surprising considering that the levels are assigned the same parity and that Blair¹¹ has successfully fitted the 18-MeV data of Seidlitz, Bleuler, and Tendam⁷ as high as 7.2-MeV excitation energy. One would thus

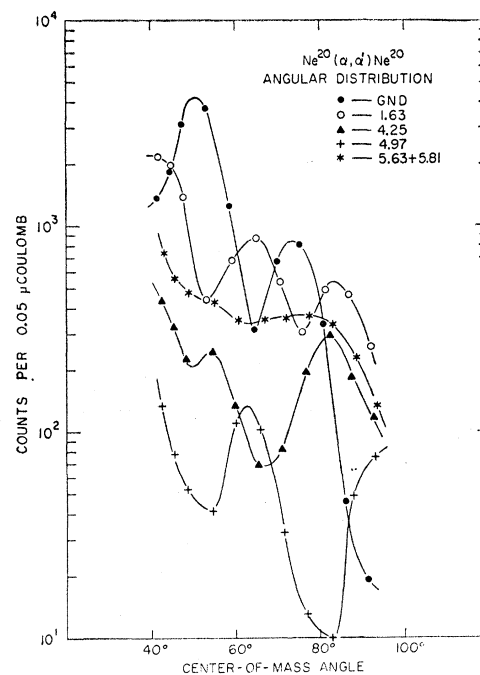


FIG. 5. Angular distribution measurements for the resolvable alpha-particle groups feeding states in Ne^{20} . Measurements are for 22-MeV alpha particles incident upon a natural neon target.

expect that at the 22-MeV alpha-particle bombarding energy used in this experiment, these two levels should oscillate very nearly in phase. If Blair's inelastic diffraction scattering model is truly applicable here, then one must assume either that there is an error in the spin assignment of one of these levels, which seems unlikely, or that there is a third unresolved level in the group which has even parity and is thus expected to be out of phase with the odd parity levels. Such an argument, without further substantiation, is weak, but the coincidence spectra will show strong evidence for the existence of a third level near 5.88 MeV, the presence of which could furnish an explanation of the smooth angular distribution observed for these levels.

B. Particle-Gamma Coincidence Spectra

Figure 6 is a gamma-ray spectrum of $\text{Ne}^{20}+\alpha$ without coincidence requirements. The energy calibration was determined through use of a Na^{22} source, and also by insertion of a C^{12} target into the gas-filled chamber immediately before and after each coincidence run; thus calibration energies of 0.511, 1.28, and 4.43 MeV were available in addition to identifiable gamma-ray lines in the spectra. The singles spectrum of Fig. 6 is featureless with the exceptions of a 0.511-MeV line, probably due to annihilation radiation, and weak evidence of a 1.63-MeV line which is expected to be the most intense of the Ne^{20} gamma rays and is the only recognizable Ne^{20} gamma ray in the spectrum. The high background is attributed to the nickel foils containing the target gas.

¹² H. E. Gove, A. E. Litherland, and M. A. Clark, Can. J. Phys. **39**, 1243 (1961).

¹³ T. H. Kruse, R. D. Bent, and L. J. Lidofsky, Phys. Rev. **119**, 289 (1960).

¹⁴ Isam Naqib, University of Washington (private communication).

¹⁵ J. A. Kuehner, Phys. Rev. **125**, 1650 (1962).

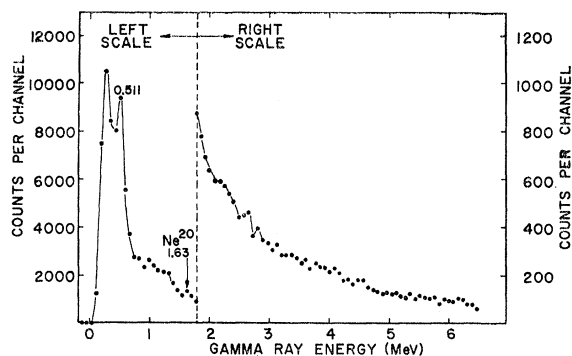


FIG. 6. Gamma-ray spectrum from the bombardment of natural neon gas with 22-MeV alpha particles. The spectrum was recorded with a 3-X3-in. NaI crystal located at 90° with respect to the beam direction.

It was clear that efficient coincidence techniques would be necessary to determine the decay modes of individual levels of Ne^{20} . The solid angle of the particle was therefore increased to about 0.4% of the total sphere (calculated for a point source). The resulting particle spectrum of $\text{Ne}^{20} + \alpha$ is shown in Fig. 7. Since the actual target was not a point, but a considerable volume of gas, the particle detector could accept particles scattered into an angular range from 30° to 60° (lab) when the detector was centered at a 40° laboratory scattering angle. This is the reason why the 1.63-MeV particle group appears at two energies in the spectrum of Fig. 7: The angular distribution of the 1.63-MeV group exhibits a sharp minimum near the center of the large angular interval accepted by the particle detector and these inelastically scattered alphas are being detected at two distinct angular regions and thus at two different energies. The peak labeled 1.63 "Ghost" is due to 1.63-MeV group particles which are detected at the extreme end of the acceptance angle near 60° (lab). Inelastic alpha particles from the 4.97-MeV level are ex-

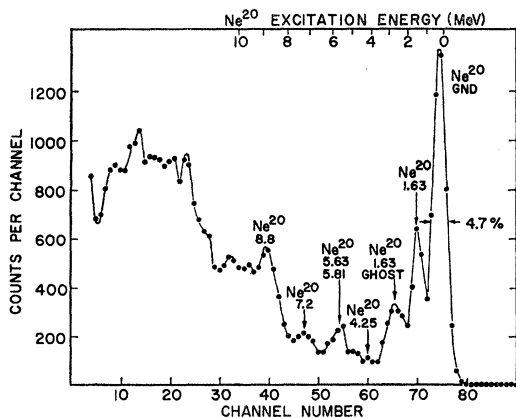


FIG. 7. Charged-particle spectrum from the bombardment of natural neon gas with 22-MeV alpha particles. Spectrum was recorded with a Hughes 1 cm^2 diffused-junction detector located at 40° with respect to the beam, and uncollimated for optimum coincidence efficiency.

pected to show a similar behavior, but are too weak to be apparent here; the other resolved groups exhibit either monotonically varying angular distributions or are sharply peaked in the acceptance interval. Energy calibration of the spectrum was accomplished by inserting a C^{12} target and a natural thorium source into the gas-filled chamber, and by correcting the positions of the observed Ne^{20} levels, using their angular distributions, so that the excitation-energy scale corresponds to a laboratory scattering at 40° which was the detector center for a point source. The particle detector was fixed at this angle for all the coincidence measurements. A detailed discussion of the energy calibration of this spectrum can be found in reference 10.

The procedure was then to systematically record gamma-ray spectra in coincidence with interesting regions of the particle spectrum. Since the resolution was not good enough to resolve all the levels of interest, calibration of the energies of the particles was accomplished by the method described in the preceding paragraph. Figures 8 and 9 clearly demonstrate that the method was working satisfactorily. Figure 8 shows the gamma-ray spectrum recorded in coincidence with alpha particles inelastically scattered to the 1.63-MeV level of Ne^{20} . The expected 1.63-MeV ground-state transition is the only line observed. Figure 9 is a gamma-ray spectrum recorded in coincidence with alpha particles inelastically scattered to the 4.25-MeV level of Ne^{20} . This spectrum shows clearcut evidence of the decay of the 4.25-MeV level through the 1.63-MeV level via a 2.62-MeV cascade gamma ray, a decay mode previously established by other experimenters.¹³

Close examination of Fig. 9 reveals that the intensity of the 1.63-MeV line is too intense to be accounted for solely by the cascade from the 4.25-MeV level. The coincidence window included some of the 1.63-MeV particle group labeled as "Ghost" in Fig. 7, so that 42% of the intensity of the 1.63-MeV line was due to direct production of 1.63-MeV level and 58% was due to the cascade transition from the 4.25-MeV level. An upper

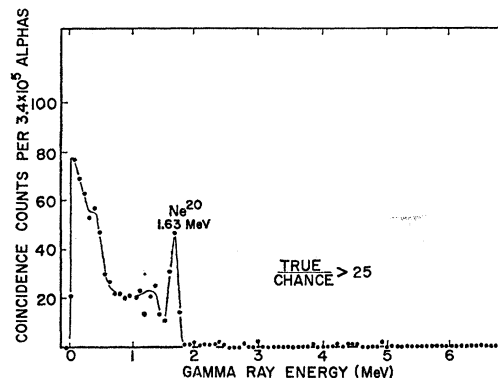


FIG. 8. Gamma-ray spectrum coincident with alpha particles inelastically scattered to levels in Ne^{20} in the excitation energy range 0.9 to 2.9 MeV. Particle detection angle = 40° . Gamma detection angle = 90° . Collection time = 3h.

limit of 3% can be placed on the ground-state transition from the 4.25-MeV level; the calculation allowed for two standard deviations in the observed counts, was corrected for pileup between the 2.62- and 1.63-MeV lines, but assumed isotropy in the distribution of the gamma rays. This estimate seems conservative and is lower than the limit of 9% obtained by Kruse *et al.*¹³

Figure 10 is a spectrum of gamma radiation which is coincident with alpha particles inelastically scattered to levels of Ne^{20} in the range 5.0 to 6.3-MeV excitation energy. The two known levels in this region at 5.63-MeV (3^-) and 5.81 MeV (1^-) have been reported by Kuehner and Almquist¹⁶ to decay predominately by alpha emission. Examination of Fig. 10 reveals the presence of four strong gamma-ray lines, three of which are clearly from the decay of Ne^{20} levels: the 1.63, 2.62, and 3.34-MeV gamma rays are due, respectively, to radiative decay of the 1.63 (2^+), 4.25 (4^+), and 4.97 (2^-) MeV levels of Ne^{20} . However, the particle window was set above these states. Some particles inelastically scattered to the 4.97 (2^-) level could satisfy the particle-energy coincidence requirement because of the poor angular resolution of the particle detection system, but inelastic alphas corresponding to the 1.63- and 4.25-MeV states were not included in this particle window; yet the absolute intensity of the 2.62-MeV line is greater in Fig. 10 than in Fig. 9 where the particle window included the 4.25-MeV state directly. Further, the intensity of the 1.63-MeV line, which cannot now be partially accounted for by direct production of the 1.63-MeV level, is twice too intense to be accounted for by cascades following the 2.62- and 3.34-MeV gamma-ray transitions. It appears that a new level near 5.88 MeV decays to the 4.25-MeV level via a 1.63-MeV line. Further evidence for the existence of this new level is presented later in the coincidence particle spectra.

The 4.0 ± 0.1 -MeV gamma ray is assigned as a cascade from the 5.63-MeV (3^-) level to the 1.63-MeV (2^+)

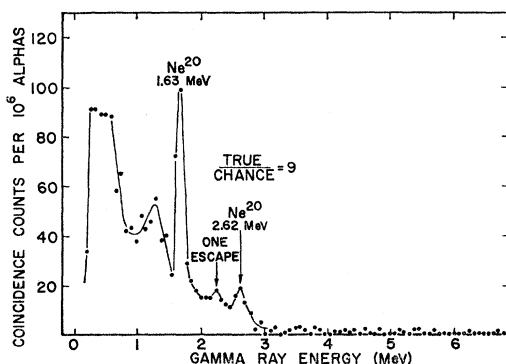


Fig. 9. Gamma-ray spectrum coincident with alpha particles inelastically scattered to levels in Ne^{20} in the excitation energy range 3.5 to 5.1 MeV. Particle detection angle = 40° . Gamma detection angle = 90° . Collection time = 7 h 37 min.

¹⁶ J. A. Kuehner and E. Almquist, Chalk River Report PD-317, 1961 (unpublished).

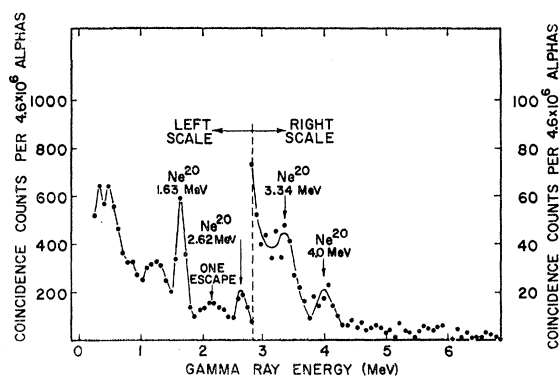


Fig. 10. Gamma-ray spectrum coincident with alpha particles inelastically scattered to levels in Ne^{20} in the excitation energy range 5.0 to 6.3 MeV. Particle detection angle = 40° . Gamma detection angle = 90° . Collection time = 33 h 17 min.

level. The energy of the line makes this assignment seem the most probable. Making peak-to-total and detector efficiency corrections,¹⁷ the intensity of the 4.0-MeV gamma ray in Fig. 10 is found to be 40% that of the directly produced 2.62-MeV gamma ray of Fig. 9. The relative intensities for production of the 4.25- and 5.63-MeV states are not known since the 5.63-MeV state is not resolved in Fig. 4. A lower limit of Γ_γ/T for the 5.63-MeV state may be obtained by assuming that the intensity of the $5.63 + 5.81 + 5.88$ sum peak is due entirely to the 5.63 alpha-particle group. Then the data are consistent with $\Gamma_\gamma/T = 0.15$ for the 5.63-MeV level. From the high intensity of the 2.26-MeV line in Fig. 10, it is clear that a large proportion of the unresolved sum peak must be due to the new 5.88-MeV level, and that the gamma width quoted above is an underestimate. Angular correlation measurements are entirely prohibitive here, since the spectrum of Fig. 10 required more than 33 h of coincidence running time to record.

Figure 11 is a gamma-ray spectrum recorded in coin-

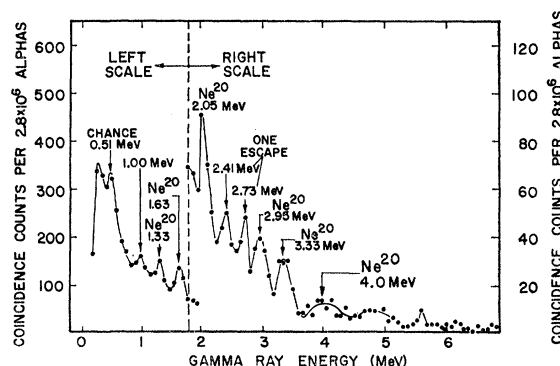


Fig. 11. Gamma-ray spectrum coincident with alpha particles inelastically scattered to levels in Ne^{20} in the excitation energy range 6.4 to 7.9 MeV. Particle detection angle = 40° . Gamma detection angle = 90° . Collection time = 18 h.

¹⁷ R. L. Heath, Atomic Energy Commission Report TID-4500 (unpublished), 13 ed.

cidence with alpha particles inelastically scattered to levels of Ne^{20} in the range 6.4 to 7.9 MeV. The only known gamma-emitting level in this region is the 7.02-MeV level which was recently discovered by Litherland, Clark, and Gove.¹⁸ The 1.33 ± 0.08 - and 2.05 ± 0.05 -MeV gamma rays are probably those reported by Litherland *et al.*¹⁸ as due to the decay of the 7.02-MeV level through the 5.63- and 4.97-MeV levels. The observed ratio for the 7.02-MeV level, 67% through the 4.97-MeV level and 33% through the 5.63-MeV level, is in agreement with the results of Litherland *et al.*¹⁸ Weaker branches to other levels may exist, but would be obscured by the complexity of the spectrum.

The presence of a 2.95 ± 0.1 -MeV line and the high intensity of the 3.34-MeV line in Fig. 11 can be explained as being due to the decay of a new level in Ne^{20} near 7.93 MeV which decays by gamma emission through the 4.97-MeV level. Presumably, since the intensity of gamma radiation from the 7.93-MeV level is comparable to that from the 7.02-MeV level, the new level must have unnatural spin and parity. Otherwise, the alpha width would be much larger than the gamma width. The assignment of the weak 1.0 ± 0.1 -MeV line in Fig. 11 is not clear and could be instrumental or possibly due to a weak branch from the new 7.93-MeV level to the 7.02-MeV level. Magnetic spectrometer measurements of the reaction $\text{C}^{12}(\text{C}^{12}, \alpha)\text{Ne}^{20*}$ by Almquist and Kuehner¹⁹ indicated the presence of a new level near

TABLE I. Assignments and intensities for observed transitions in Ne^{20} .

| Excitation interval in Ne^{20} | Gamma-ray energy (MeV) | Gamma-ray counts per 1×10^6 elastically scattered alphas | Transition assignment |
|---|------------------------|---|---|
| $\alpha' 0.9-2.9$ (Fig. 8) | 1.63 ± 0.04 | 1230 | $\text{Ne}^{20}(1.63 \rightarrow 0)$ |
| $\alpha' 3.5-5.1$ (Fig. 9) | 1.63 ± 0.05 | 450 | $\text{Ne}^{20}(1.63 \rightarrow 0)$ (from 1.63 "ghost") |
| | 2.62 ± 0.10 | 290 | $\text{Ne}^{20}(4.25 \rightarrow 1.63 \rightarrow 0)$ $\text{Ne}^{20}(4.25 \rightarrow 1.63)$ |
| $\alpha' 5.0-6.3$ (Fig. 10) | 1.63 ± 0.05 | 820 | $\text{Ne}^{20}(5.88 \rightarrow 4.25)$ $\text{Ne}^{20}(5.88 \rightarrow 4.25 \rightarrow 1.63 \rightarrow 0)$ $\text{Ne}^{20}(4.97 \rightarrow 1.63 \rightarrow 0)$ $\text{Ne}^{20}(5.63 \rightarrow 1.63 \rightarrow 0)$ |
| | 2.62 ± 0.05 | 360 | $\text{Ne}^{20}(5.88 \rightarrow 4.25 \rightarrow 1.63)$ |
| | 3.34 ± 0.02 | 60 | $\text{Ne}^{20}(4.97 \rightarrow 1.63)$ |
| | 4.00 ± 0.10 | 120 | $\text{Ne}^{20}(5.63 \rightarrow 1.63)$ |
| | | | |
| $\alpha' 6.4-7.9$ (Fig. 11) | 1.33 ± 0.08 | 60 | $\text{Ne}^{20}(7.02 \rightarrow 5.63)$ |
| | 1.63 ± 0.05 | 230 | $\text{Ne}^{20}(7.02 \rightarrow 4.97 \rightarrow 1.63 \rightarrow 0)$ $\text{Ne}^{20}(7.93 \rightarrow 4.97 \rightarrow 1.63 \rightarrow 0)$ |
| | 2.05 ± 0.05 | 120 | $\text{Ne}^{20}(7.02 \rightarrow 4.97)$ |
| | 2.95 ± 0.10 | 80 | $\text{Ne}^{20}(7.93 \rightarrow 4.97)$ |
| | 3.33 ± 0.10 | 210 | $\text{Ne}^{20}(7.02 \rightarrow 4.97 \rightarrow 1.63)$ $\text{Ne}^{20}(7.93 \rightarrow 4.97 \rightarrow 1.63)$ |
| | 4.0 ± 0.2 | 30 | $\text{Ne}^{20}(7.02 \rightarrow 5.63 \rightarrow 1.63)$ |

¹⁸ A. E. Litherland, M. A. Clark, and H. E. Gove, Can. J. Phys. **39**, 1249 (1961).

¹⁹ E. Almquist and J. A. Kuehner, Can. J. Phys. **39**, 1246 (1961).

7.93 MeV, but the presence of the 7.93-MeV alpha group at 0° scattering angle implied that the level they observed had spin and parity $(-1)^J$ and would not thus seem to be the source of the gamma radiation observed in this experiment.

There seems to be clear evidence of a weak 4.0-MeV gamma ray in the spectrum of Fig. 11. This transition can only be assigned as due to decay of the 5.63-MeV level which, in this case, is being fed by the 1.33-MeV gamma-ray transition from the 7.02-MeV level. Taking into account peak-to-total ratios and efficiencies for a 3-in. \times 3-in. NaI crystal,¹⁷ a conservative estimate of the intensity of the 4.0-MeV line indicates that approximately 50% of the decay of the 5.63-MeV level can be accounted for by the 4.0-MeV gamma-ray transition. Assuming that the only production of the 5.63-MeV level is through the 1.33-MeV cascade from the 7.02-MeV level and that gamma-gamma correlation effects are small, the data imply a value $\Gamma_\gamma/\Gamma=0.5$, but with large uncertainties. These data, together with

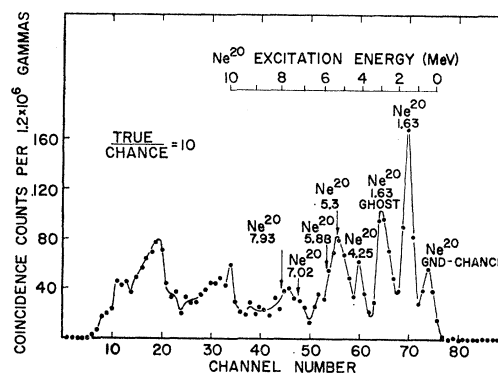


Fig. 12. Charged-particle spectrum coincident with 1.3- to 2.0-MeV gamma radiation. Particle detection angle = 40° . Gamma detection angle = 90° . Collection time = 6 h 25 min.

the analysis of Fig. 10, give a value of $\Gamma_\gamma/\Gamma=0.3 \pm 0.2$ for the 5.63-MeV level. This is significantly larger than the value of $\Gamma_\gamma/\Gamma=0.07 \pm 0.01$ reported by Kuehner and Almquist.¹⁶

Table I is a summary of the observed gamma-ray energies and the assignments of these transitions for the various coincidence spectra shown previously. The intensities in each case have been normalized to 1×10^6 elastically scattered alpha particles. The coincidence runs were normalized to one another by simply monitoring the yield of elastic alpha particles; this method was found to be highly stable over the long coincidence runs and was actually necessary since the beam was stopped within the gas-filled chamber and accurate integration was difficult. For all the gamma rays shown in Table I, peak-to-total corrections were made from the tables of Heath¹⁷ and detector efficiency corrections were made on the observed intensities normalizing to the efficiency of the detector for 1.63-MeV gamma radiation which was present in all spectra. All measurements

were made with the gamma detector at 90° and the particle detector at 40° with respect to the beam direction, and thus the intensities quoted are for this one angular position; the yield was too low for further angles to be investigated.

In order to make the assignments more conclusive, particle spectra were recorded in time coincidence with gamma rays of selected energy intervals. Figure 12 is a particle spectrum (to be compared with the singles spectrum of Fig. 7) taken in coincidence with 1.3- to 2.0-MeV gamma rays. All particle groups feeding levels which decay through the 1.63-MeV level and/or decay by gamma radiation of such an energy that it would be accepted by the coincidence energy requirement should be present in this spectrum. In addition to the expected groups feeding the 1.63-MeV level and its "ghost" peak and the group feeding the 4.25-MeV level, a rather intense group is observed centered around 5.3 MeV and is presumably a mixture of particles feeding the 4.97-, 5.63-, and 5.88-MeV levels. There seems to be weaker

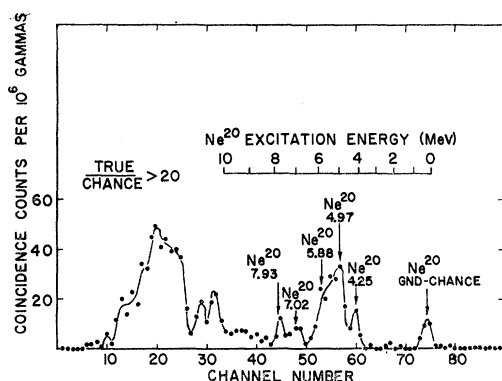


FIG. 13. Charged-particle spectrum coincident with 2.4- to 3.0-MeV gamma radiation. Particle detection angle = 40° . Gamma detection angle = 90° . Collection time = 4 h 36 min.

evidence of groups feeding the 7.02- and 7.93-MeV levels.

Figure 13 is a particle spectrum taken in coincidence with 2.4- to 3.0-MeV gamma radiation. As expected, the 1.63 and 1.63 "ghost" particle groups have completely disappeared. Particle groups feeding levels at 4.25, 4.97, 5.88, 7.02, and 7.93 MeV are clearly in evidence. This spectrum presents rather strong evidence for the existence of levels with large gamma widths lying between the 4.97- and 7.02-MeV levels. Since the particle group feeding the 4.97-MeV level is much weaker than the group feeding the 4.25-MeV level at this angle, it is assumed that the very intense, broad peak labeled 4.97 and 5.88 MeV in Fig. 13 is due primarily to particle groups feeding the 5.63- and 5.88-MeV levels. This interpretation is consistent with the analysis of the gamma-ray spectra presented earlier in this paper.

Figure 14 is a particle spectrum taken in coincidence with 3.2- to 4.0-MeV gamma radiation. Particle groups

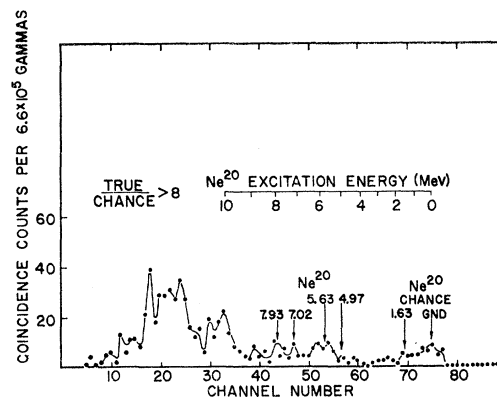


FIG. 14. Charged-particle spectrum coincident with 3.2- to 4.0-MeV gamma radiation. Particle detection angle = 40° . Gamma detection angle = 90° . Collection time = 4 h.

feeding levels which decay through the 4.97-MeV level and/or emit higher-energy gamma rays should be present in this spectrum. There is very slight (if any) evidence of the particle group feeding the 4.97-MeV level, but there is strong evidence of a group centered about 5.63-MeV excitation energy. Since all the gamma radiation associated with the decay of the new 5.88-MeV level is lower in energy than the coincidence energy interval, no particle group feeding the 5.88-MeV level can be included. Thus, the broad peak at 5.63 MeV must be due entirely to particles populating the 5.63-MeV level. Comparison with the angular distribution measurements of Fig. 5 indicates again that Γ_γ/Γ for the 5.63-MeV level must be considerably larger than earlier reported by Kuehner and Almquist,¹⁶ and that this data is consistent with the value obtained from the gamma-ray spectra. Further evidence for the levels at 7.02 and 7.93 MeV is as expected, since these levels are thought to decay through the 4.97-MeV level.

The particle spectra recorded in coincidence with gamma rays of selected energies all qualitatively reinforce the interpretation of the coincidence gamma-ray spectra. Particle spectra recorded in coincidence with higher energy gamma radiation are less interesting with respect to the low-lying levels discussed earlier in this paper and are not presented here; however, weak evidence was observed of a particle group feeding a level near 7.26-MeV excitation energy, which possibly could be the unnatural parity level observed by Rabson *et al.*²⁰ to decay by gamma emission directly to the ground state. No evidence for this particle group is seen in the particle spectra discussed in the preceding paragraphs, confirming Rabson's report that the primary mode of decay of the 7.26-MeV level is through a direct ground state transition.

Figure 15 summarizes the results of the coincidence spectra in an energy-level diagram of Ne^{20} . Gamma-emitting levels studied in this experiment are indicated by heavy lines. Only gamma-ray transitions observed in this experiment are shown. Spin and parity assign-

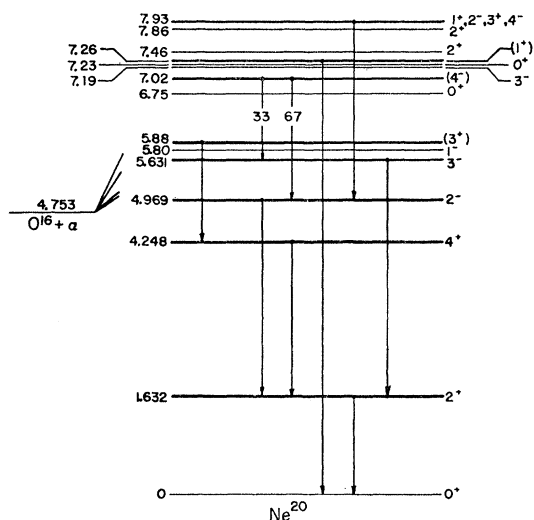


FIG. 15. Energy levels of Ne^{20} . The gamma-emitting levels studied in the present experiment are indicated by heavy lines.

ments are taken from recent investigations as indicated in the text of this paper and from the compilation of Ajzenberg and Lauritsen.⁶

IV. DISCUSSION

The angular distribution measurements shown in Fig. 5 indicate that the spin and parity of the new gamma-emitting state at 5.88 MeV are probably not 1^- , 3^- , or 5^- , since such states could be strongly excited by a direct interaction mechanism and would be expected to be in phase with the 3^- , 5.63-MeV and 1^- , 5.80-MeV states. A 0^- state cannot be formed by inelastic alpha scattering. If the 4.25-MeV state is 4^+ and we assume that the $5.88 \rightarrow 4.25$ -MeV transition is dipole or electric quadrupole, then 0^+ , 1^+ , and 2^- assignments for the 5.88-MeV state are ruled out. A 2^+ assignment for the 5.88-MeV level seems unlikely, since for this assignment it is expected that Γ_γ/Γ would be small. These arguments leave 3^+ as the most likely assignment for the 5.88-MeV level, though higher spin assignments such as 4^\pm and 5^+ are also possible. Similar arguments suggest 1^+ , 2^- , 3^+ , or 4^- as possible assignments for the 7.26-MeV state reported by Rabson, *et al.*²⁰

The gamma-emitting states at 5.88 MeV (3^+), 7.26 MeV (1^+), and 7.93 MeV (1^+ , 2^- , 3^+ , 4^-) are not in-

cluded in the rotational band scheme proposed by Litherland *et al.*⁴ To fit these levels into a collective model with rotational bands, new rotational bands of even parity must be proposed. It is possible that the 3^+ state at 5.88 MeV is a three-phonon quadrupole vibrational state. The second-phonon excitation then would be identified with the state at 4.25 MeV. It was pointed out in Sec. III A (c) that the angular distribution of alpha particles corresponding to the 4.25-MeV state was not in exact accord with the Blair phase rule. Recent calculations by Buck²¹ indicate that this anomaly may arise from an interference effect between direct and multiple transition mechanisms for exciting the first 4^+ state. The nonaxial model of Davydov and Filippov²² can also account for a low-lying 3^+ state at 5.88 MeV; however, this model then requires a 2^+ assignment for the 4.25-MeV state. Recent experiments of Gove, Litherland, and Clark¹² indicate a 4^+ assignment for the 4.25-MeV state.

Several unnatural-parity [$\pi \neq (-1)^J$] levels of Ne^{20} were produced in the present experiments. The 4.97-MeV (2^-) level was also observed in the 18-MeV Ne^{20} (α, α') studies of Seidlitz, Bleuler, and Tendam.⁷ However, the 5.22-MeV 3^+ level in Mg^{24} was produced with very low intensity by 42-MeV inelastic alpha-particle scattering.¹⁴ Presumably, if the process is purely direct, the mechanism which produces unnatural parity levels in 0^+ ground-state nuclei is one in which a spin-orbit interaction between the orbital angular momentum of the incident alpha-particle and the spin of one (or more) nucleons in the target nucleus causes an odd number of target nucleons to undergo a spin-flip. An alternative explanation for the production of unnatural parity levels is that the interaction proceeds through a double scattering of the alpha particle. Detailed experiments at various alpha-particle bombarding energies would provide interesting information concerning the energy dependence of the mechanism which produces unnatural parity states.

ACKNOWLEDGMENTS

The authors are grateful to Professor M. Ross for informative theoretical discussions, to R. A. LaSalle for assistance in recording the data, to Professor M. B. Sampson for suggestions on efficient cyclotron operation, and to Professor A. C. G. Mitchell for his encouragement and support.

²¹ B. Buck, Phys. Rev. **127**, 940 (1962), and private communication.

²² A. S. Davydov and G. F. Filippov, Nuclear Phys. **8**, 237 (1958).

²⁰ T. A. Rabson, W. D. Barfield, D. L. Bernard, T. W. Bonner, and W. W. Givens, Nuclear Phys. **21**, 43 (1960).